Hindawi
Advances in Civil Engineering
Volume 2018, Article ID 1569271, 12 pages
https://doi.org/10.1155/2018/1569271

Research Article

Variation of Velocity Distribution in Rough Meandering Channels

Arpan Pradhan,[1] **Kishanjit Kumar Khatua**,[2] **and Sovan Sankalp**[3]

[1]*Department of Civil Engineering, Hydraulics Laboratory, National Institute of Technology Rourkela, Rourkela, Odisha, India*
[2]*Department of Civil Engineering, National Institute of Technology Rourkela, Rourkela, Odisha, India*
[3]*Department of Civil Engineering, Remote Sensing and GIS, National Institute of Technology Rourkela, Rourkela, Odisha, India*

Correspondence should be addressed to Arpan Pradhan; er.arpanpradhan@gmail.com

Received 20 August 2017; Revised 28 January 2018; Accepted 26 February 2018; Published 1 April 2018

Academic Editor: Giuseppe Oliveto

Distribution of flow and velocity in a meandering river is important in river hydraulics to be investigated from a practical point of view in relation to the bank protection, navigation, water intakes, and sediment transport-depositional patterns. When flow enters a bend, the centrifugal force arising from the channel curvature leads to a transversal slope in the water surface. The interaction between the centrifugal force and transversal pressure gradient causes secondary flows in cross-sections, and the secondary flows spread further by moving along the bend. Hence, at the bends, these processes lead to longitudinal velocity increase in the inner wall and decrease at the outer wall. In this paper, experimentation is carried out for two different bed roughness on a 4.11 sinuosity meandering channel with 110° crossover. Longitudinal velocity distribution is analysed with the graphical illustrations for the detailed experimental study. Study of flow profile across the crossover is also particularly important as the inner bank of the bend changes to the outer bank and vice versa which has a significant effect on the water surface profile and hence on the velocity distribution along the full meander path. The objective of the analysis is to determine the effect of curvature and roughness on the velocity profiles, throughout the meander path. It is determined that the resistance of flow, on the smoother bed channel, is higher than that of the channel with higher Manning's n above a certain depth at the apex and transition sections. A reciprocal study of the experimental investigation is attempted with a numerical hydrodynamic tool, namely, CCHE (Centre for Computational Hydroscience and Engineering) developed by NCCHE, University of Mississippi, US. The model is applied to simulate the inbank flow velocity distribution and validate the experimental observation for the meandering channel with rough bed.

1. Introduction

Distribution of velocity varies along the depth as well as the width of the channel. The variation along the depth ranges from zero at the channel bed to a maximum value, either at the water surface or at a distance below it, reliant on the channel characteristics. This nonuniformity in the velocity distribution is affected predominantly by the bed shear stresses. Flow turbulence structures are influenced by the roughness or smoothness of the channel boundary; consequently, making roughness and shear to be dominant factors influencing the velocity distribution. On considering the width of the channel, it is observed that for straight channels, the velocity is maximum at the central region. Such flow characteristics, although seen in straight channels, is not observed in meandering channels. Meandering of a channel is quantified by sinuosity or the crossover angle. Sinuosity is calculated by the ratio of the curved distance traveled by the channel with respect to straight distance. The crossover angle on the other hand is the angle made by the crossover and the bend apex sections.

Flow in meandering channels is quite ambiguous. In general, rivers hardly flow straight and uniform. They are always seen in a typical curved or meandering form. Rivers generally follow this pattern for minimization of energy loss. Meandering channels are equilibrium features that represent

the most probable plan geometry, where single channels deviate from straightness. Information regarding the nature of flow in simple and compound meandering channels is needed to solve a variety of river hydraulics and engineering problems such as to give a basic understanding of the flow attributes, to understand the mechanism of sediment transport, and to design stable channels.

Considerable research on various aspects of velocity distribution in curved meandering rivers has been carried out, but no systematic effort has been made to analyze the variation of velocity profile along a meander path [1]. Flow characteristics and velocity distributions in meandering rivers are essential issues to be investigated in the field of river hydraulics from a practical point of view in relation to the bank protection, navigation, water intakes, and sediment transport-depositional patterns. Knowledge on velocity distribution of a channel also helps to determine the energy expenditure, bed shear stress distribution, and the associated heat and mass transport problems.

Extensive studies on flow characteristics in channels have been carried out with different bend angles by using experimental and numerical models. Blanckaert and Graf [2] while investigating the channel bed level changes for a 120° sharp bend with a movable bed reported a minor secondary rotating flow cell at the outer wall of the bend. Shiono et al. [3] developed turbulence models and studied the behavior of secondary flows and centrifugal forces for straight and meandering channels. McKeogh and Kiely [4] studied velocity distribution in meandering compound channels and stated that the maximum velocity in main channel, whether above or below the bank level, is closer towards the inner bend. Similar observation was made by Sellin and Willets [5], also showing that the velocity weakens and moves across to the outside of the bend while moving further downstream. He et al. [6] studied a similar flow pattern and formulated a nonlinear model to simulate the flow pattern and the evolution of meandering channels. A limitation to their formulation is that the model did not perform well for highly meandering channels. Akbari and Vaghefi [7] provided experimental investigation on a 180° sharp bend, for streamlines of longitudinal profiles, cross sections, and plans. Although, it is not meandering channel, but the results at the maximum curvature were analogous to a bend apex. Therefore, experimental study on the velocity variation in a highly meandering channel was necessitated. Few literature is available on meandering channels with higher bed roughness particularly the detailed comparison of longitudinal velocity between different roughness. Hence, the present study incorporated the experimental investigation on two differently roughened meandering channels with high sinuosity. The variation of longitudinal velocity for both the channels is studied in detail for a complete meander path.

Numerical hydraulic models significantly reduce cost associated with the experimental models, and their use has been rapidly expanded in the recent decade. Booij [8] and Van Balen et al. [9] modeled the flow pattern at a mildly curved 180° bend and assessed the secondary flow structure using large eddy simulation (LES). Zhou et al. [10] using the two-dimensional depth-averaged model, simulated the flow pattern in 180° sharp bend and 270° mild bend, with and without consideration of the secondary flow, and claimed that, given the effect of the secondary flow, the simulation results in the first state have a better agreement with the experimental results. Naji Abhari et al. [11] studied the flow pattern in a 90° mild bend numerically and experimentally, focusing on the velocity distributions, the streamlines at different water levels, and the distribution of shear stresses. The results showed that the flow pattern in a channel bend is heavily influenced by the secondary flow and centrifugal force. Bonakdari et al. [12] investigated the flow pattern at a 90° mild bend using the numerical model, artificial neural network, and genetic algorithm. Khatua et al. [13] studied the evaluation of roughness coefficients in meandering channels. Mohanty [14] anticipated lateral depth-averaged velocity distribution in a trapezoidal meandering channel, and a quasi-1D model Conveyance Estimation System (CES) was applied to the same meandering channel to analyse the depth-averaged velocity.

CCHE2D (National Center for Computational Hydroscience and Engineering's 2-Dimensional Model) is a two-dimensional depth-averaged, unsteady flow, and sediment transport model in which the flow model is based on depth-averaged Navier–Stokes equations. This is an integrated package for simulation and analysis of free surface flows, sediment transport, and morphological processes. Hossain et al. [15] examination approves the CCHE2D hydrodynamic model flood replication results utilizing a progression of satellite imagery and a few advanced digital image processing procedures. Kim [16] studied the changes in the bed of the Geum River in South Korea by using the CCHE2D model. Li et al. [17] studied the transport of flow and bed load in a 110° sine-generated laboratory meandering flume by applying CCHE2D.

In this paper, experimental investigation is performed to study the velocity distributions in a highly meandering channel of sinuosity 4.11 with 110° crossover angle for both smooth and rough channel beds. The velocity profiles are analyzed to find the flow pattern and movement of the local maximum velocity at different sections along the meander path in-between two successive bend apex regions. The CCHE2D model is utilized to compare the depth-averaged velocity variation along the meander path.

2. Methodology

Langbein and Leopold [18] suggested that the shape of meanders is comparable to sine-generated functions. This function can be utilized in determining a continuous variation in curvature of the centerline as preferred for forming an ideal natural meander wave evolution phase. A sine-generated curve being specified by the value of the deflection angle, θ_o, at the point of inflection, the channel sinuosity can be evaluated by the first kind Bessel function of zeroth order [19]. Basing on this concept, an experimental meandering channel with a sine-generated curvature is constructed having a 110° deflection angle with two and half meander wavelengths. The wavelength for the meandering channel was set as 2.162 m with a 4.11 sinuosity. The experimental

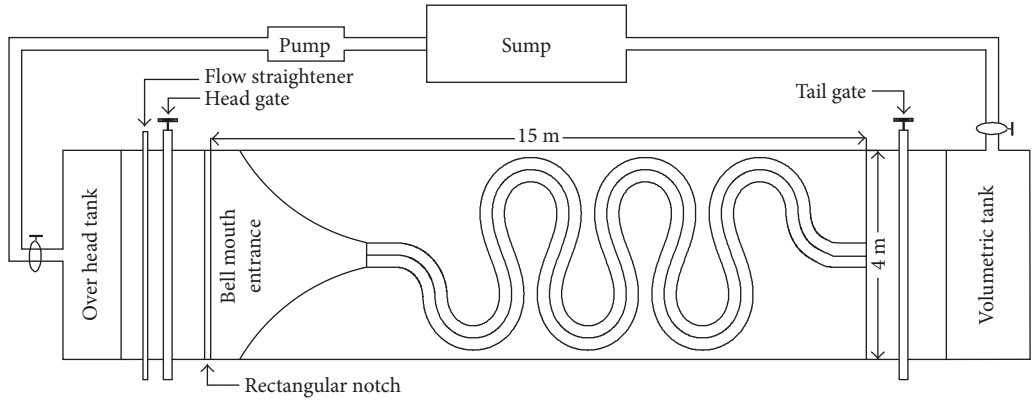

Figure 1: Planform of the experimental setup for the the meandering channel.

(a) (b)

Figure 2: Experimental meandering channels: (a) smooth and (b) rough.

channel is constructed over a cast iron flume of width 4 m and length 15 m.

2.1. Experimental Setup. Experimental investigations are conducted in the highly meandering trapezoidal channel at NIT, Rourkela. The channel has a side slope of 1 : 1 with 0.33 m as the bottom width and 0.065 m as the bank-full depth, the valley slope being 0.00165. The plan for the experimental process is demonstrated in Figure 1. Research in the proposed experimental channel is carried out with two different roughness, denoted as smooth and rough.

Smooth refers to the channel constructed with the Perspex sheet, with an assumed height of 0.1 mm. However, rough refers to a channel with 1.2 mm gravels fixed to the bed. The basis of denoting this roughness as smooth and rough is illustrated in Section 2.3. The setup for both these types is illustrated in Figure 2.

Manning's roughness is dependent upon various factors including channel geometry and sinuosity and not just the bed material [20–22]. Therefore, calculation of Manning's n for the bed material is not appropriate on meandering channels. Hence, Manning's n value for the above materials is determined on a straight rectangular channel, which are found to be 0.01 and 0.014 for the Perspex and gravel beds, respectively.

Individual discharges of 5 l/s and 5.2 l/s are maintained for the Perspex and gravel bed meandering channels, respectively. These individual discharges provide an equivalent value of the aspect ratio (b/h) in the channels at every section along the meander path so as to aid in comparison of the velocity variations.

2.2. Test Sections. Observations are recorded along a meander path, that is, between two consecutive bend apex regions. For the present experimental study, the region between the second and third bend apex is taken into consideration. The assessments are undertaken at different reaches along the prescribed path as demonstrated in Figure 3(a). The channel has a crossover angle of 110°. Hence, the sections in the meander path are resolved by dividing the crossover angle into six equal sectors on either side of the crossover region with respect to the centerline of the channel. Perpendicular sections to both the channel boundaries for each of the sector lines are drawn to provide thirteen sections including the two bend apex sections, A and M, and the crossover section G. Figure 3(b) shows the grid positions for measurement of longitudinal velocity for each of the sectional reaches using a series of the Pitot tubes in assistance of a moving bridge arrangement.

Measurements are taken across the main channel in the direction of flow. The lateral spacing of the grid points has

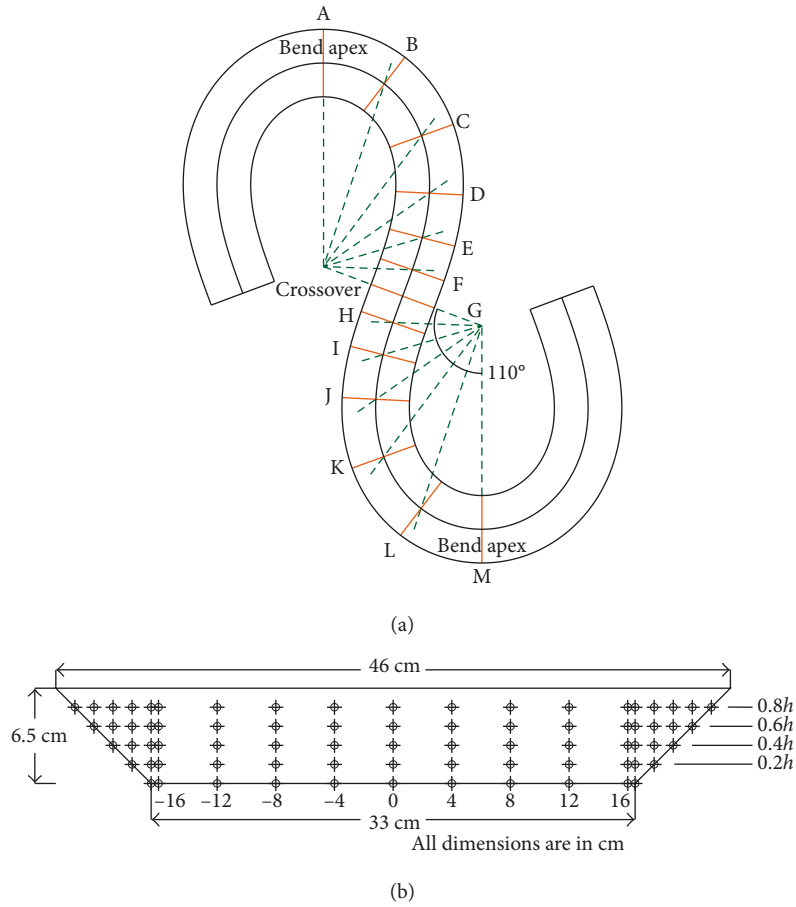

Figure 3: (a) Test section. (b) Position of measurement.

been taken as 4 cm on either side of the centerline. The depth of flow at any individual section is not constant in the case of a meandering channel. The lateral spacing on the bank region is dependent upon the individual depth of flow, for the particular section. As the trapezoidal channel has a 1 : 1 side slope, the lateral distance is proportional to the vertical distance, demarcated as $0.2h$, $0.4h$, $0.6h$, and $0.8h$.

Tail gate on the rear end of the flume is adjusted for maintaining a constant water depth of around 0.05 m, throughout the meander path. This is done for both the cases of meandering channels.

2.3. Theoretical Consideration. Influence of the shape and bed roughness has an enormous effect on the velocity distribution of a channel. Friction velocity or bed shear velocity is a significant term in the context of computing the velocity profile as well as for determining the bed roughness. Friction velocity u^* is defined as the fluid velocity at an elevation of $z = z_0 e^{\kappa}$, where z_0 is the elevation at zero velocity and κ is the von Kármán constant equal to 0.4.

The apparent elevation for zero velocity, that is, z_0, primarily depends upon the flow characteristic of the channel, that is, the kinematic viscosity, friction velocity, and roughness height. A classification for the value of z_0 has been provided by Nikuradse and Liu [23, 24], suggesting different formulations for hydraulically smooth, rough, and transition flows. Te Chow [25] suggested the friction velocity to be defined as

$$u^* = \sqrt{\frac{\tau_0}{\rho}}, \tag{1}$$

where τ_0 is the bed shear stress and ρ is the density of the fluid.

$$\tau_0 = \rho g h S, \tag{2}$$

where h is the depth of flow and S denotes the surface or bed slope. The friction velocity can thus be defined as

$$u^* = \sqrt{ghS}. \tag{3}$$

The friction velocity of a channel can then be used to determine the flow condition, that is, whether the flow occurs over a hydraulically smooth or rough surface. Hydraulically smooth refers to the flow over surface irregularities submerged completely in the laminar sublayer [25]; hence, the velocity distribution is unaffected by the bed roughness. Hydraulically rough refers to flow over large surface irregularities which produce eddies at the bed. In this case, viscous sublayer is absent, and hence, the velocity distribution is solely affected by the bed roughness. Yalin [19], Graf [26], and Schlichting and Gersten [27] suggested classification for such channels by the means of friction velocity u^* (m/s) as depicted below:

$$0 < \frac{u^* k}{\nu} < 5, \tag{4}$$

$$5 < \frac{u^* k}{\nu} < 70, \tag{5}$$

$$70 < \frac{u^* k}{\nu}. \tag{6}$$

where k refers to the roughness height in meter and ν is the kinematic viscosity (m^2/s) of the fluid flow. Equation (4) refers to the condition of flow over a hydraulically smooth bed, while (5) and (6) denote flow over transition region and hydraulically rough surfaces, respectively.

Velocity distribution plots over a transition region are affected by the bed roughness as well as viscosity [25]. The roughness height for the Perspex sheet and the gravel are determined as 0.0001 m and 0.012 m, respectively. The kinematic viscosity of water was taken as 1.14×10^{-6} m^2/s with an average value of u^* being 0.01396 m/s and 0.01385 m/s for the smooth and rough beds, respectively. The average values of $(u^* k/\nu)$ are hence calculated to be in the ranges of 1.225 and 145.835 for the Perspex and gravel beds, respectively. In the current study of velocity distribution, the bed roughness is demarcated as smooth and rough by the use of the above classifications. Friction velocity, u^*, at the elevation z, respective to the bed roughness is obtained and is used in portraying the velocity distribution plots.

2.4. Numerical Analysis Using CCHE2D. The CCHE2D model is based on depth-averaged Navier–Stokes equations, and the depth-integrated two-dimensional equations are generally accepted for studying the open channel hydraulics in shallow flow conditions with reasonable accuracy and efficiency. These equations include the momentum equations and the continuity equations. In addition to the numerical model itself, this family includes two more members: a mesh generator (CCHE2D mesh generator) and a graphical users interface (CCHE2D-GUI). The CCHE2D mesh generator allows the rapid creation of complex-structured mesh systems for the CCHE2D model with several integrated useful techniques and methods. The CCHE2D-GUI is a graphical user's environment for the CCHE2D model with four main functions: preparation of initial and boundary conditions, preparation of model parameters, run numerical simulations, and visualization of modelling results. The momentum equations for depth-integrated two-dimensional turbulent flows in a Cartesian coordinate system are

$$\frac{du}{dt} + u\frac{du}{dx} + v\frac{du}{dy} = -g\frac{dz}{dx} + \frac{1}{h}\left[\frac{d(h\tau_{xx})}{dx} + \frac{d(h\tau_{xx})}{dx}\right] - \frac{\tau_{xy}}{\rho h} + f_{\text{cor}} v, \tag{7}$$

$$\frac{dv}{dt} + u\frac{dv}{dx} + v\frac{dv}{dy} = -g\frac{dz}{dx} + \frac{1}{h}\left[\frac{d(h\tau_{xx})}{dx} + \frac{d(h\tau_{xx})}{dx}\right] - \frac{\tau_{by}}{\rho h} + f_{\text{cor}} u, \tag{8}$$

where u and v are the depth-integrated velocity components in x and y directions, respectively; t is the time; g is the acceleration due to gravity and ρ is the density; h is the local water depth; f_{cor} is the Coriolis parameter; and τ_{xx}, τ_{yy}, and τ_{yx} are the depth-integrated Reynolds stresses. Free surface elevation for the flow is calculated by the depth-integrated continuity equation:

$$\frac{\partial \zeta}{\partial t} + \frac{\partial uh}{\partial x} + \frac{\partial vh}{\partial y} = 0. \tag{9}$$

Assuming the bed elevation, ζ, would not change in the flow simulation process $\partial\zeta/\partial t = 0$, the continuity equation is then simplified to

$$\frac{\partial \eta}{\partial t} + \frac{\partial uh}{\partial x} + \frac{\partial vh}{\partial y} = 0, \tag{10}$$

where η is the free surface elevation and h is the water depth. Because bed morphological change is a much slower process than hydrodynamics, this equation is widely accepted and utilized for computing free surface with two-dimensional models.

The mesh represents a computational domain where the governing equations are discretized. Therefore, for successful simulation, the regions should have proper resolution with the inlets and outlets sufficiently further from each other. The computations are conducted in a limited portion of the free surface flow; hence, the boundary conditions are the driving mechanism with which the flow in the simulated area behaves. Therefore, the boundary conditions should be provided as close to the physical conditions as possible. The numerical simulation is carried out to reproduce true physics by solving mathematical equations.

3. Results and Discussion

3.1. Experimental Observation. The variation in velocity is represented as a nondimensional parameter, that is, as u/u^*, where u^* is the bed shear velocity or friction velocity corresponding to the individual channel condition and u is the longitudinal point velocity at the particular grid point. This nondimensional velocity variation is plotted against the inverse aspect ratio, $\alpha' = h/b$. The inverse aspect ratio has been considered so as to give a nondimensional factor in the velocity variation study. Therefore, with similar aspect ratios, the velocity distribution across a section in both smooth and rough meandering channels can be analyzed together.

Variation of longitudinal velocity at the 13 undertaken sections is illustrated in Figures 4–16, with a comparison of the variations with respect to roughness of the channel. Figures 4 and 16 represent the bend apex sections A and M, respectively, whereas Figure 11 is the crossover section G. Figures 5–9 and 11–15 represent the five intermediate sections in between each of the bend apexes and the crossover.

On observing the profiles across a cross section, it is seen that the velocity remains higher towards the inner wall for both the cases of bed roughness. The highest velocity for a particular section gradually moves from the outer wall on

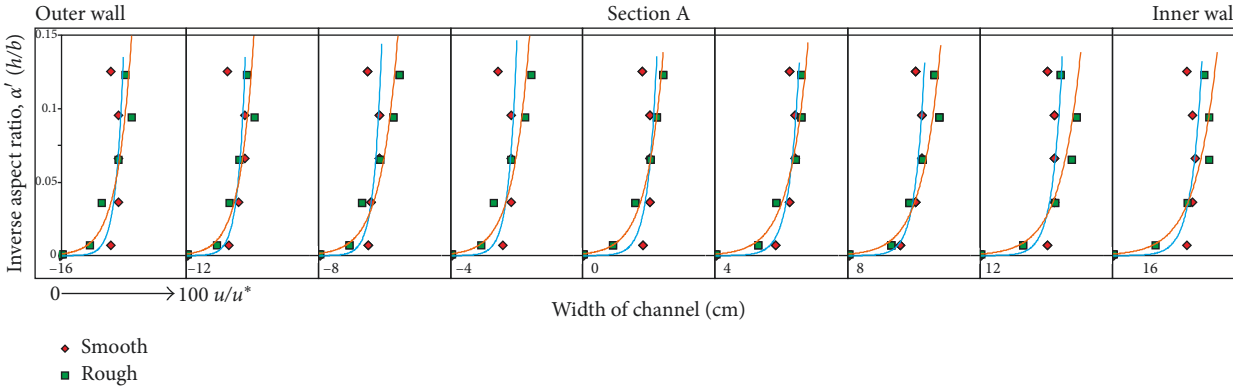

Figure 4: Comparison of velocity variation in section A.

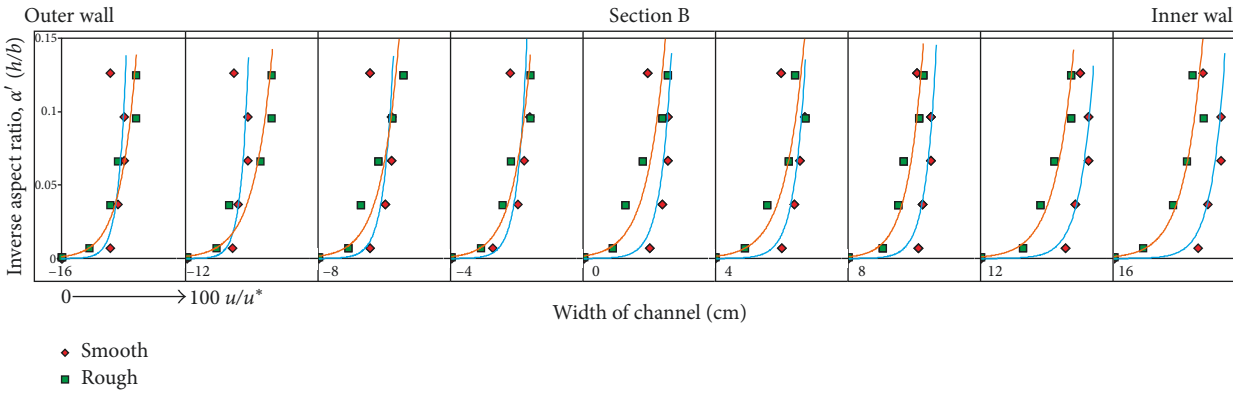

Figure 5: Comparison of velocity variation in section B.

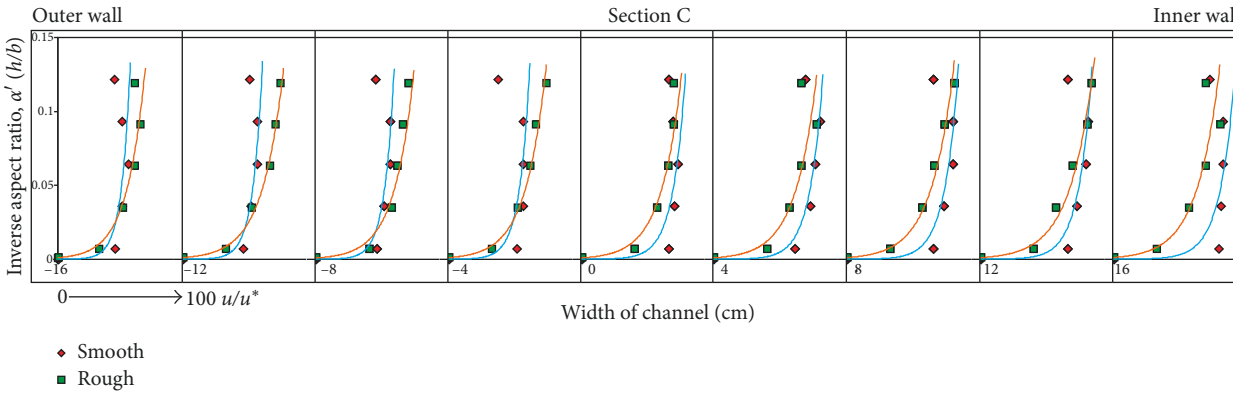

Figure 6: Comparison of velocity variation in section C.

the left-hand side of section A (Figure 5) towards the central region of crossover section G, as seen in Figure 10. The highest velocity on moving further downstream is observed to move to the right-hand side of the adjoining bend apex section M as seen in Figure 16. The transition in the movement of the maximum velocity from the channel sides to the center of crossover, for a meander path, occurs at the intermediate sections D and J.

In a straight channel, an increase in bed roughness would imply higher value of Manning's n and therefore lower velocity. Such an observation should also have been possible in the case of a meandering channel. But, as observed in Figure 4, that is, bend apex section A, the longitudinal velocity in the rough meandering channel is lower than its smoother counterpart only up to a depth of $0.2h$ to $0.4h$. As the depth increases, the velocity distribution in the rough meandering channel is observed to be higher than that in the smoother. Therefore, this indicates that there is a greater resistance on the smoother channel, above this depth. The only other effect is the curvature, which is same for both the channels. It is concluded that the resistance caused due to the meandering effect is more on the smoother channel. It is

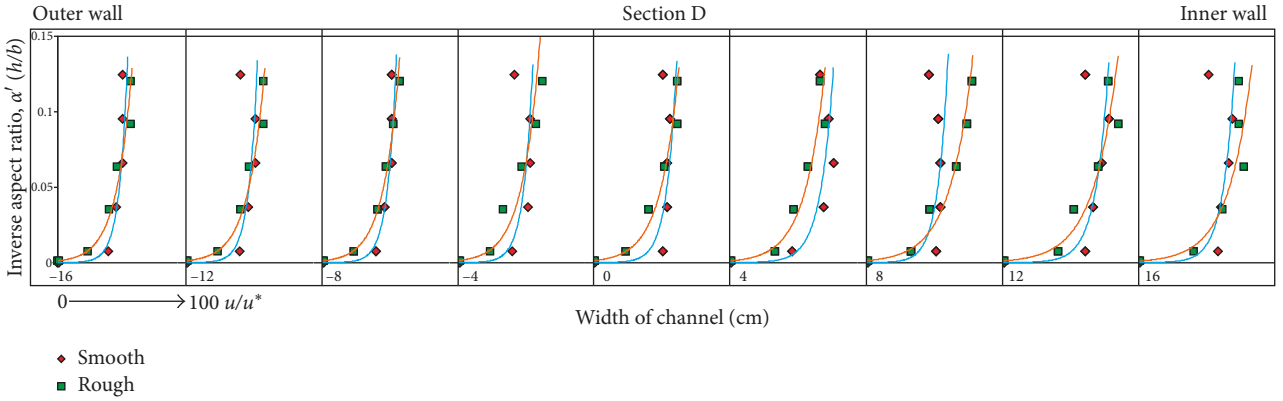

Figure 7: Comparison of velocity variation in section D.

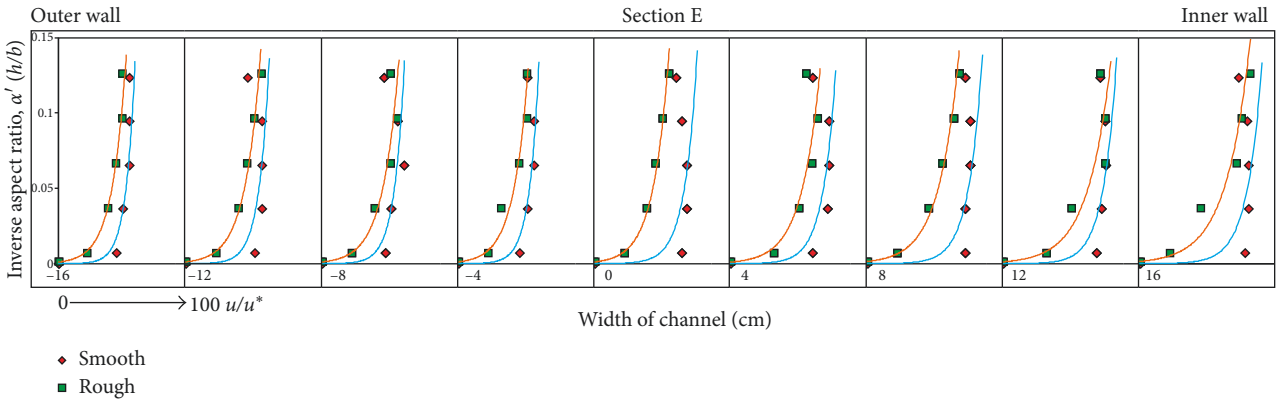

Figure 8: Comparison of velocity variation in section E.

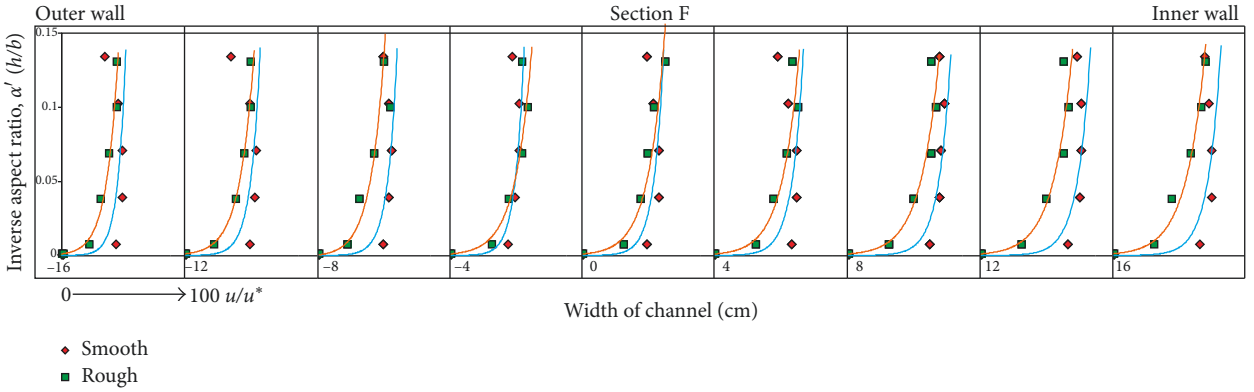

Figure 9: Comparison of velocity variation in section F.

hence deduced that the curvature of the channel has a significant effect on the velocity variation and not just the bed roughness. Such an observation is consistent across the channel section for both the bend apexes A and M as seen in Figures 4 and 16, respectively.

At the sections following the apexes, sections B to F and sections H to L, that is, up to the crossover, the overlapping of the velocity profiles for the different roughness is only observed around the outer regions. At the inner banks, the velocity variation in the smooth and rough bed meandering channels is seen to be distinctly apart. The only exception is the transition sections D and J (Figures 7 and 13). The observation at these sections is quite synonymous to the apex, with the overlaying of the profiles occurring at a depth of around $0.4h$ to $0.6h$. Such an observation can be attributed to the movement of maximum velocity from the inner wall of the bend apex towards the central region of the crossover.

In the crossover section (Figure 10), the velocity profiles for both the roughness are distinctly apart, throughout the

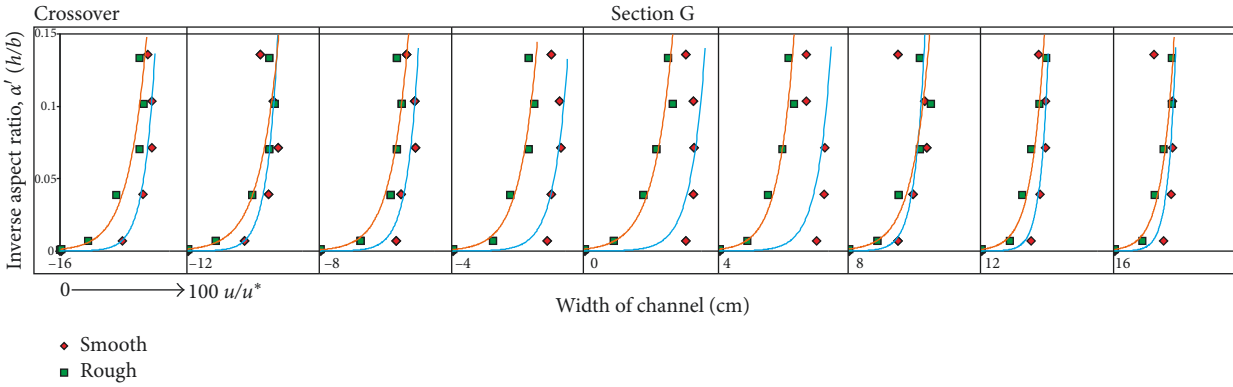

Figure 10: Comparison of velocity variation in section G.

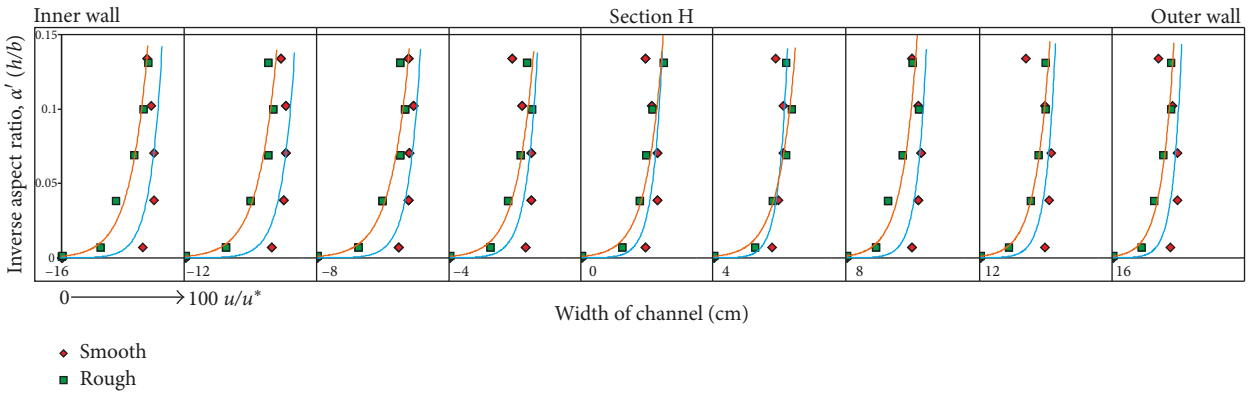

Figure 11: Comparison of velocity variation in section H.

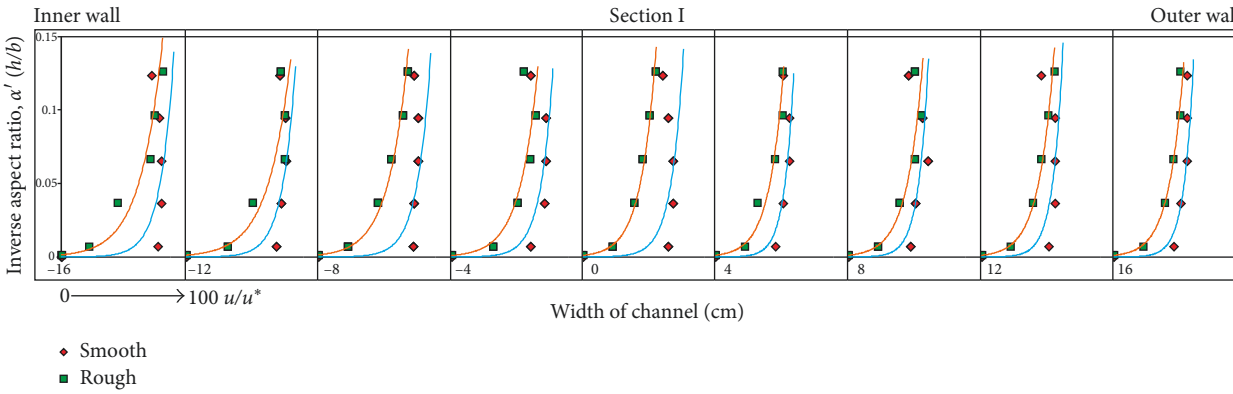

Figure 12: Comparison of velocity variation in section I.

cross section. Longitudinal velocity in the rough bed is seen to be lower in magnitude than that in the smoother channel across the cross section. The higher cross-sectional velocity is also observed to be at the center. Such observation is similar to a straight channel, for which it is deduced that the crossover section behaves as a straight channel.

3.2. Simulation by CCHE2D. In the CCHE mesh interface, the experimental meandering channel is drawn providing it with a structured and orthogonal mesh. The outer boundaries of the channel are first drawn such that the intermediate sections are perpendicular to both the boundaries, as seen in Figure 17(a). More number of nodes are drawn at the meander bends for better discretization. Figure 17(b) represents the optimized mesh with an initial bed elevation.

The parameters for the CCHE mesh and GUI are provided in Table 1. The CCHE2D model is developed for the experimental rough meandering channel. In the GUI, the bed roughness and an initial water depth are provided as initial conditions. Manning's n value of 0.014 is provided as the bed roughness. An initial water depth is

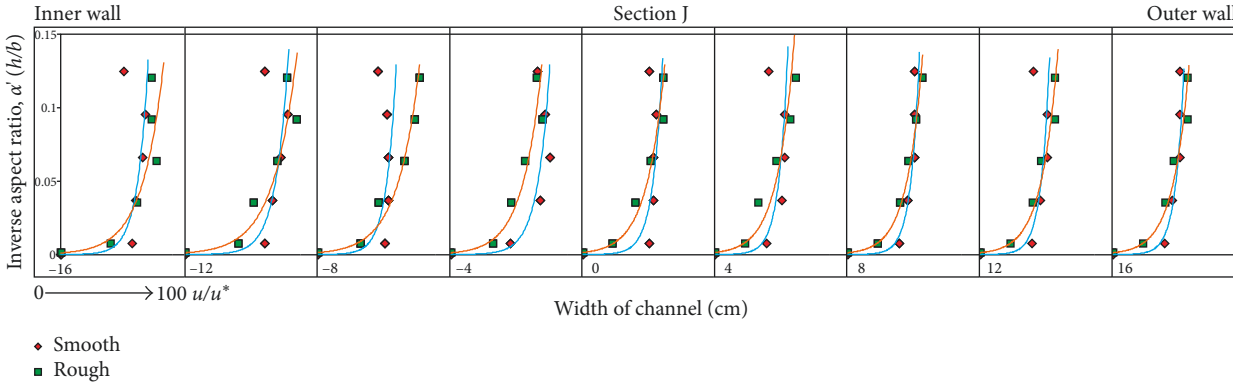

Figure 13: Comparison of velocity variation in section J.

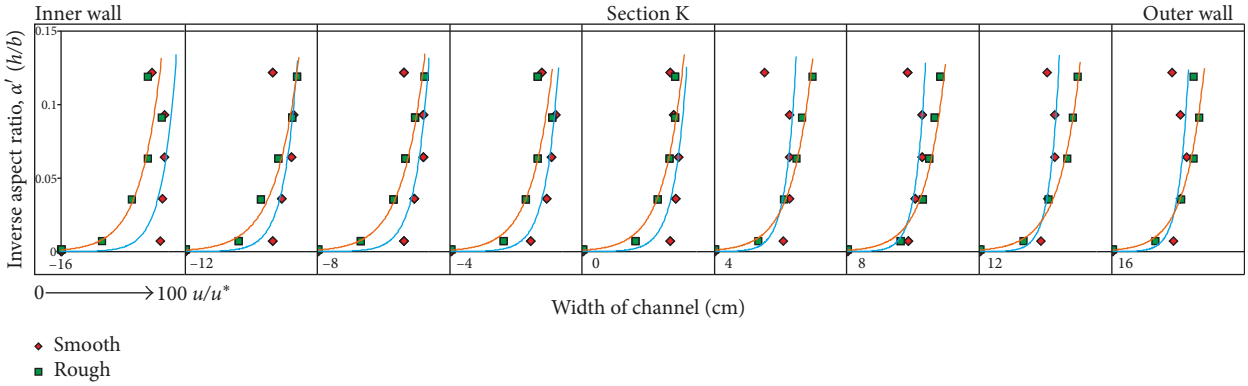

Figure 14: Comparison of velocity variation in section K.

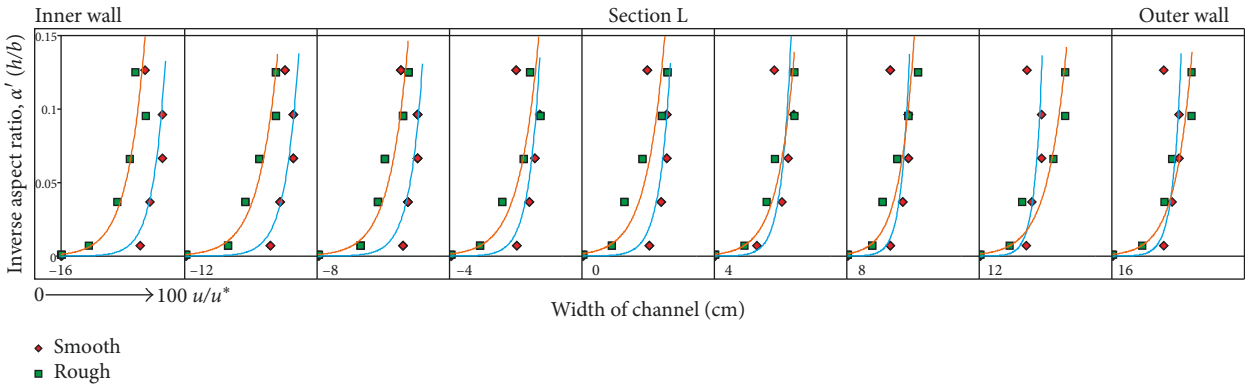

Figure 15: Comparison of velocity variation in section L.

a requisite for the model to initiate the iteration. Therefore, a small water depth of 0.01 m is provided as the initial water surface.

The boundary conditions in the CCHE2D model are the inlet discharge and the outlet water depth. The inlet discharge is provided as 5.2 l/s, similar to that of the experimentation. As denoted in Section 2.2, the average depth of flow for the entire meander path between the second and third bend apex is around 0.05 m. This depth is maintained by adjusting the tail gate to form a quasi-uniform flow. By leaving the tail gate open, the flow depth would naturally fall, which is also predicted in the case of the CCHE2D model. Hence, 0.03 m depth of flow is provided as the boundary condition at the outlet, so as to maintain an average depth of 0.05 m at the region between the second and third bend apex.

Figure 18(a) represents the simulation result of CCHE2D for depth-averaged distribution, whereas Figure 18(b) represents the experimental observation of average velocity assumed to occur at $0.4h$. The meander path taken into consideration is illustrated as the region between the sections demarcated as A and M on both the insets.

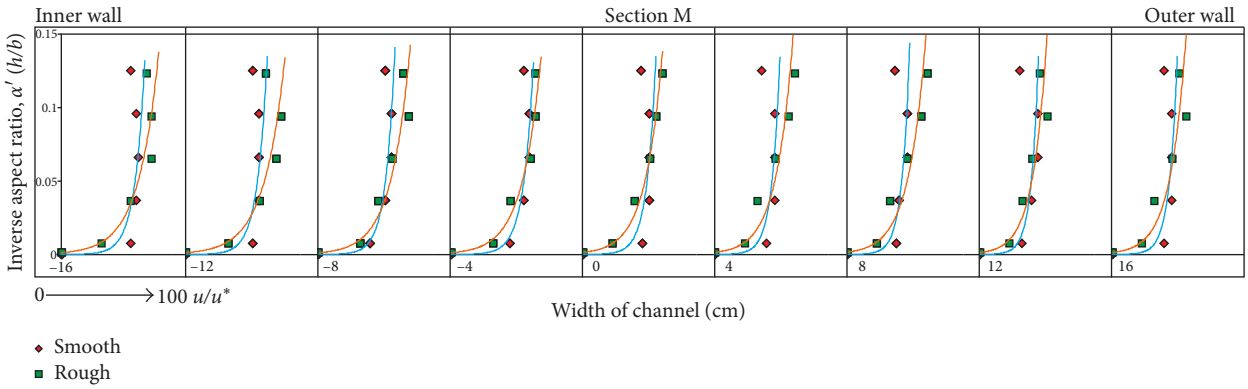

Figure 16: Comparison of velocity variation in section M.

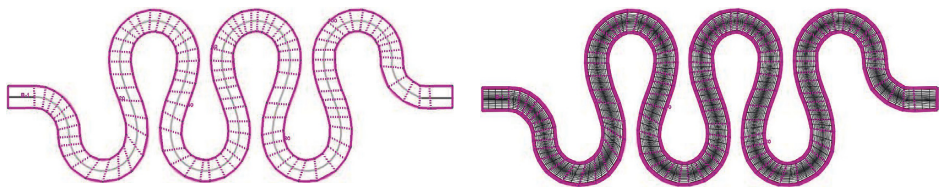

Figure 17: CCHE mesh: (a) construction of the channel boundary and (b) meshing for the entire channel.

Table 1: Condition set for the numerical model.

Serial number	CCHE mesh	CCHE GUI
1	$I_{max} = 24$ and $J_{max} = 500$	Initial bed elevation = 0.065 m
2	Number of iterations = 10	Bed roughness, n = 0.014
3	Smoothing parameter = 0.5, B-spline	Initial water surface = 0.01 m
4	Exponential parameter, E = contract	Inlet boundary condition = 0.0052 $m^3 \cdot s^{-1}$
5	Deviation parameter, $D = 0.5$	Outlet boundary condition = 0.03 m
6	Smoothing parameter, $S = 3.5$	

The maximum velocity for the experimental observation (i.e., Figure 18(b)) at sections A and M is found to be around 100 cm/s. From the simulation results of CCHE2D, the maximum value at these sections is seen to be in the range of 0.998 m/s which is quite close to the experimental observations.

In Figure 18(a), the velocity distribution along the meander path is observed to decrease uniformly up to the crossover section, which then gradually increases towards the next consecutive bend apex, much similar to what is observed in Figure 18(b) for the experimental study. The degree of variation in this above observation is also quite similar, which can be determined from the contours.

The velocity values around the crossover region are observed to be negative in the contour index of Figure 18(a). It is pertinent to mention that the negative sign is due to the direction of flow and not a negative velocity. The direction of longitudinal velocity, for instance, the crossover section, is slightly towards the left. Since the longitudinal velocity is taken as positive in the x-axis of the first quadrant for the CCHE2D model, these values are represented with a negative sign.

There is a slight difference in the CCHE2D model prediction for the depth-averaged velocity around the crossover region in comparison with the experimental study. The crossover region has a depth-averaged velocity of around 12 cm/s for the experimental channel, which is predicted to be 18 cm/s by CCHE2D. From the above analysis, it can be suggested that CCHE2D to some extent is capable of predicting the depth-averaged velocity distribution in experimental meandering channels.

4. Conclusions

In this paper, an experimental investigation is carried out to observe the velocity distribution plots for two meandering channels with different roughness beds. The analysis is carried out to find the effect of bed roughness and curvature of the meandering channel on the velocity variations. The velocity distributions are found to remain higher towards the inner wall of the sections, in and around the bend apex region of the meander path. This observation is distinctively similar for both the bed roughness.

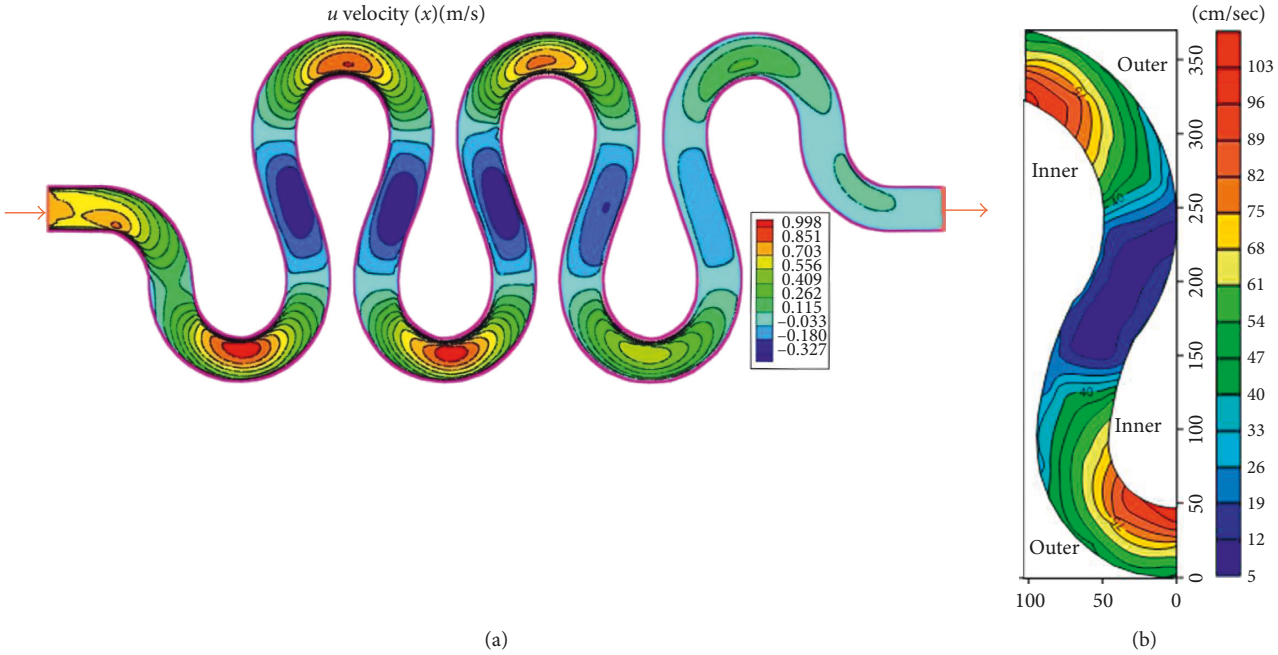

Figure 18: Depth-averaged velocity distribution: (a) CCHE2D simulation and (b) experimental.

At the meander bends, above the depth of $0.2h$ to $0.4h$, the resistance caused by the curvature of the channel is found to be more on a smoother channel than that on a rough channel with same geometric conditions. Similar observations are found in sections, at the middle of the apexes and the crossover sections in a meander path, but above a depth of about $0.4h$ to $0.6h$. These observations can be attributed to the position of maximum curvature at the bend apexes (A and M) and the movement of maximum velocity from the inner wall of the bend apex towards the central region of the crossover at sections D and J. The longitudinal velocity profiles at the crossover section G are found to be following similar patterns to that of straight channels.

In the numerical analysis done by CCHE2D, it can be concluded that the longitudinal velocity, that is, the u velocity, as considered by the software observes maximum velocity at the inner side of the bend apex region which is synonymous to the experimental velocity contour diagram. On comparing the experimental analysis with the numerical analysis, it was found that the maximum velocity values as calculated and observed in both the cases have a very minute variation. It can be therefore deduced that CCHE2D to some extent is capable of predicting the depth-averaged velocity distribution in experimental meandering channels.

It is deduced, from the present experimental analysis, that the effect of curvature is more on a smoother channel above a certain depth at the bend apex and the transition sections. Future scope of the study would be to analyse the extent of this curvature by experimentations on meandering channels with different curvatures.

Conflicts of Interest

The authors declare that they have no conflicts of interest.

References

[1] A. Pradhan, K. K. Khatua, and S. S. Dash, "Distribution of depth-averaged velocity along a highly sinuous channel," *Aquatic Procedia*, vol. 4, pp. 805–811, 2015.

[2] K. Blanckaert and W. H. Graf, "Mean flow and turbulence in open-channel bend," *Journal of Hydraulic Engineering*, vol. 127, no. 10, pp. 835–847, 2001.

[3] K. Shiono, Y. Muto, D. W. Knight, and A. F. L. Hyde, "Energy losses due to secondary flow and turbulence in meandering channels with overbank flows," *Journal of Hydraulic Research*, vol. 37, no. 5, pp. 641–664, 1999.

[4] E. J. McKeogh and G. K. Kiely, "Experimental study of the mechanisms of flood flow in meandering channels," in *Proceedings of the 23rd IAHR Congress*, pp. 491–498, Ottawa, Canada, August 1989.

[5] R. H. J. Sellin and B. B. Willets, "Three-dimensional structures, memory and energy dissipation in meandering compound channel flow," *Floodplain Processes*, pp. 255–298, Wiley, Chichester, UK, 1996.

[6] L. He, D. Chen, K. Blanckaert et al., "Modeling flow pattern and evolution of meandering channels with a nonlinear model," *Water*, vol. 8, no. 12, 2016.

[7] M. Akbari and M. Vaghefi, "Experimental investigation on streamlines in a 180 sharp bend," *Acta Scientiarum Technology*, vol. 39, no. 4, p. 425, 2017.

[8] R. Booij, "Measurements and large eddy simulations of the flows in some curved flumes," *Journal of Turbulence*, vol. 4, no. 1, pp. 1–17, 2003.

[9] W. Van Balen, W. S. J. Uijttewaal, and K. Blanckaert, "Large-eddy simulation of a mildly curved open-channel flow," *Journal of Fluid Mechanics*, vol. 630, pp. 413–442, 2009.

[10] G. Zhou, H. Wang, X. Shao, and D. Jia, "2-D numerical simulation of flow in a curved open channel," in *Proceedings of the Advances in Water Resources and Hydraulic Engineering-16th IAHR-APD Congress and 3rd Symposium of IAHR-ISHS*, pp. 871–876, Nanjing, China, October 2009.

[11] M. Naji Abhari, M. Ghodsian, M. Vaghefi, and N. Panahpur, "Experimental and numerical simulation of flow in a 90° bend," *Flow Measurement and Instrumentation*, vol. 21, no. 3, pp. 292–298, 2010.

[12] H. Bonakdari, S. Baghalian, F. Nazari, and M. Fazli, "Numerical analysis and prediction of the velocity field in curved open channel using artificial neural network and genetic algorithm," *Engineering Applications of Computational Fluid Mechanics*, vol. 5, no. 3, pp. 384–396, 2011.

[13] K. K. Khatua, K. C. Patra, and P. Nayak, "Meandering effect for evaluation of roughness coefficients in open channel flow," *WIT Transactions on Ecology and the Environment*, vol. 146, pp. 213–224, 2011.

[14] P. K. Mohanty, *Flow Analysis of Compound Channel with Wide Flood Plains*, Ph.D. thesis, National Institute of Technology, Rourkela, India, 2013.

[15] A. K. M. A. Hossain, Y. Jia, and X. Chao, "Validation of CCHE2D model using digital image processing techniques and satellite imagery," in *Proceedings of the 33rd IAHR Congress*, Vancouver, Canada, August 2009.

[16] Z. Kim, *Assessment of Riverbed Change due to the Operation of a Series of Gates in a Natural River*, Ph.D. thesis, Texas A&M University, College Station, TX, USA, 2013.

[17] H. Li, D. Chen, Y. Jia, and Y. Zhang, "Modeling bedload transportation along the same-side and opposite banks of meaders," in *E-Proceedings of the 36th IAHR World Congress*, Hague, Netherlands, July 2015.

[18] W. B. Langbein and L. B. Leopold, *River Meanders-Theory of Minimum Variance*, US Government Printing Office, Washington, DC, USA, 1966.

[19] M. S. Yalin, *River Mechanics*, Elsevier, New York, NY, USA, 1992.

[20] A. Pradhan and K. K. Khatua, "Assessment of roughness coefficient for meandering compound channels," *KSCE Journal of Civil Engineering*, pp. 1–13, 2017, In press.

[21] H. Azamathulla, Z. Ahmad, and A. Ghani, "An expert system for predicting Manning's roughness coefficient in open channels by using gene expression programming," *Neural Computing and Applications*, vol. 23, no. 5, pp. 1343–1349, 2013.

[22] A. Pradhan and K. K. Khatua, "Gene-expression programming to predict Manning's n in meandering flows," *Canadian Journal of Civil Engineering*, 2018, In press.

[23] J. Nikuradse, *Laws of Flow in Rough Pipes*, National Advisory Committee for Aeronautics, Washington, DC, USA, 1950.

[24] Z. Liu, *Sediment Transport*, Aalborg Universitet, Aalborg, Denmark, 2001.

[25] V. Te Chow, *Open Channel Hydraulics*, McGraw-Hill Book Company Inc., New York, NY, USA, 1959.

[26] W. H. A. Graf, *Fluvial Hydraulics: Flow and Transport Processes in Channels of Simple Geometry*, Wiley, New York, NY, USA, 1998.

[27] H. Schlichting and K. Gersten, *Boundary Layer Theory*, Springer-Verlag, Berlin, Heidelberg, Germany, 2000.